Available online at www.sciencedirect.com
ScienceDirect
Journal of Power Sources 158 (2006) 1419–1424
JOURNAL OF POWER SOURCES
www.elsevier.com/locate/jpowsour

Short communication

Particle size effects on temperature-dependent performance of $LiCoO_2$ in lithium batteries

Sun Hee Choi [a], Ji-Won Son [a], Young Soo Yoon [b], Joosun Kim [a,*]

[a] *Nano-Materials Research Center, Korea Institute of Science and Technology, P.O. Box 131, Cheongryang, Seoul 130-650, Republic of Korea*
[b] *Department of Advanced Fusion Technology, Konkuk University, 1 Hwayang-dong, Gwangjin-gu, Seoul 143-701, South Korea*

Received 14 June 2005; accepted 14 October 2005
Available online 2 December 2005

Abstract

The effect of the particle size of $LiCoO_2$ on the operating temperature-dependent performance of lithium batteries is investigated. The $LiCoO_2$ particle size is successfully controlled by modifying the powder preparation process and well-controlled nanocrystalline $LiCoO_2$ powders are obtained. It is found that the discharge capacity of a cell made with the nanocrystalline powder is slightly lower than that of cells made with micron-sized powders. On the other hand, the cycle performance of the cell using nanocrystalline $LiCoO_2$ powder is consistent over the selected operating range of temperature (−15 to 60 °C) without deterioration. It is concluded that the smaller size of the particles contributes to the enhancement of the reliability by increasing the specific surface-area for intercalation sites, and by enhancing the resistance to mechanical failure especially at higher temperatures.

Keywords: Lithium cobalt oxide; Lithium-ion battery; Temperature-dependent performance; Nanocrystalline powder; Particle size effect

1. Introduction

$LiCoO_2$ has been widely studied as a cathode material for lithium batteries since it has a longer cycling life than that of other candidates such as $LiNiO_2$ and $LiMn_2O_4$. Preparation of $LiCoO_2$ is commonly undertaken by heat-treatment at above 700 °C. This method yields high temperature (HT) $LiCoO_2$, which is reported to exhibit better properties than those of its low-temperature counterpart [1–4]. Conventionally, $LiCoO_2$ cathodes are fabricated based on powder processing using micron-sized particles. Since the performance of batteries depends significantly on the microstructure of the cathode and this, in turn, depends on the starting powder, it is important to control the size of the precursor particles and investigate its effect on cell performance.

For commercial applications, batteries are typically expected to operate at various temperatures. Hence, it is important to achieve the performance reliability over a wide temperature range. It has been reported [5] that the low-temperature performance of lithium batteries is limited mainly by the electrolyte solution, which determines the ionic mobility between the electrodes. Generally, the specific energy and power of Li-ion batteries are substantially reduced as the temperature falls below −10 °C because the ionic mobility decreases in the electrolyte solution. Hence, electrolyte solutions with a low melting point, such as propylene carbonate, are used for batteries operating at low temperature [5]. On the other hand, the employment of a fabrication process that can compensate the reduction in the ionic mobility (e.g., one that increases the surface-area of electrodes by using nano-scale powders) can be of a particular interest.

Along with the low-temperature performance, reliable high-temperature performance of batteries is also important since cells cycled with currents greater than 2*C* experience an internal temperature of more than 38 °C [6]. The large increases in cell impedance with both cycling and ageing at elevated temperature are attributed to several causes that include the formation of a non-uniform solid electrolyte interface (SEI) layer and electrolyte decomposition [7]. Also, mechanical stress induced during phase transition of the cathode material at high temperature can be detrimental to cell performance.

This study is based on the assumption that the reliability of cell performance at various operating temperatures can

* Corresponding author. Tel.: +82 2 958 5528; fax: +82 2 958 5529.
E-mail address: joosun@kist.re.kr (J. Kim).

0378-7753/$ – see front matter © 2005 Elsevier B.V. All rights reserved.
doi:10.1016/j.jpowsour.2005.10.076

be enhanced by using nanocrystalline $LiCoO_2$ powders (n-$LiCoO_2$). The intercalation sites can be increased by using n-$LiCoO_2$ due to the increased specific surface-area. Also, nanocrystalline powders are thought to be more resistant to mechanical stress or failure because of their minute size. Thus, an investigation has been made of the effect of particle size on cell performance at various temperatures. The particle sizes of $LiCoO_2$ are successfully controlled by combining salt encapsulation with a conventional powder processing technique [8–10] and nanocrystalline and micron-sized $LiCoO_2$ powders are obtained. By analyzing the electrochemical behaviour of cells fabricated with these powders and a commercial powder, the particle-size dependent cell performance is examined and probable underlying physical reasons are discussed.

2. Experimental

To fabricate n-$LiCoO_2$ powders, an aqueous solution of Li and Co acetates (Li/Co = 1.1) was frozen by spraying it on liquid nitrogen. The solution was then freeze-dried for 2 days at $P = 5 \times 10^2$ mbar. A 1:10 mixture of the freeze-dried product and K_2SO_4 was prepared, and ball-milled in a planetary mill (Pulverisette-5, Fritsch) for 24 h (ZrO_2 ball to powder mass ratio = 10:1). Because $LiCoO_2$ particles are encapsulated with K_2SO_4 by this process, coarsening of the $LiCoO_2$ was prevented. A two-step thermal decomposition of the mixture was performed consequently in air by holding the mixture at 400 °C for 10 h, then at 800 °C for 12 h. After washing the thermally processed mixture in distilled water several times to eliminate SO_4^{2-} ions, the $LiCoO_2$ was separated by centrifugation.

To characterize the obtained n-$LiCoO_2$ powders, X-ray diffraction (XRD, Geigerflex, Rigaku, 2° min^{-1}, Cu Kα) and scanning electron microscopy (SEM, Philips ESEM) were used. For comparing the performance of the nano-sized and micron-sized powders, commercially available micron-sized $LiCoO_2$ powders (SELION C-012, Seimi Co., Japan) and fabricated coarse-grained powders were also investigated. The fabrication procedure for coarse-grained powders was the same as that of nanocrystalline powders except for mixing with K_2SO_4.

To investigate cell performances, CR2032 coin-type cells were constructed with each type of powders. Cathode materials were prepared by mixing 20 mg of each type of $LiCoO_2$ powder and 12 mg of a conductive binder (8 mg acetylene black and 4 mg graphite). The mixture was pressed under a pressure of 300 kg cm^{-2} on a 200 mm^2 stainless-steel mesh that acted as a current-collector, then this structure was dried at 180 °C for 24 h in a vacuum oven. A porous polypropylene film (Celgard 3401) was used for separating the cathode and a lithium metal anode, and a mixture of 1 M $LiPF_6$-ethylene carbonate/dimethyl carbonate (1:1, v/v, Merck) was used as the electrolyte. After constructing the coin cell, electrochemical properties such as the discharge capacity and the cycle performance were characterized at various operating temperatures of −15, −10, −5, 0, 25, 40, 50 and 60 °C. Impedance spectra were also measured by means of an impedance analyzer (SI 1287 and SI 1260, Solartron, USA). The frequency was varied from 5 mHz to 100 kHz with an ac oscillation of 30 mV. While measuring the impedance spectra, a dc bias voltage was matched to the open-circuit voltage (OCV) of the cell.

3. Results and discussion

Scanning electron microscopic analysis of the $LiCoO_2$ powders obtained by K_2SO_4 encapsulation confirmed that the method efficiently prevents grain coarsening. The commercially available powder (Fig. 1A) and that without K_2SO_4 encapsulation (Fig. 1B) consist of micron-sized particles, while the particle size of the powder obtained by using K_2SO_4 (Fig. 1C) is in the range of 30–70 nm. X-ray diffraction analysis of micron-sized powders (Fig. 2A and B) and of nanocrystalline powder (Fig. 2C) reveals the formation of single-phase hexagonal HT-$LiCoO_2$ in both cases. Heat-treatment of $LiCoO_2$ powders at 800 °C in contact with K_2SO_4 does not show reflections from

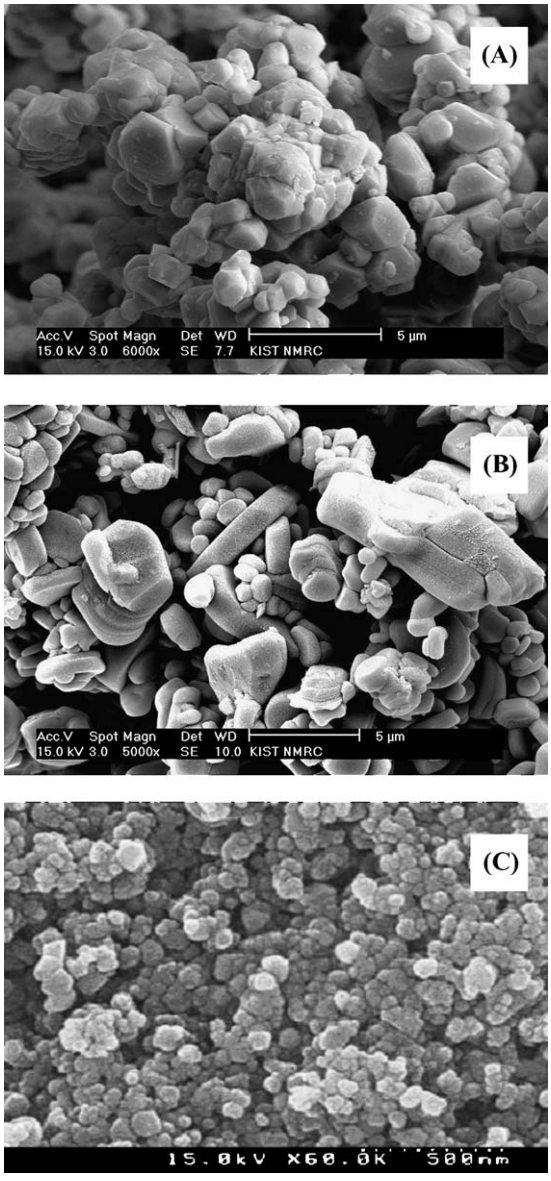

Fig. 1. Scanning electron micrographs of $LiCoO_2$: (A) commercial powder; (B) manufactured coarse-grained powder; (C) encapsulated with K_2SO_4.

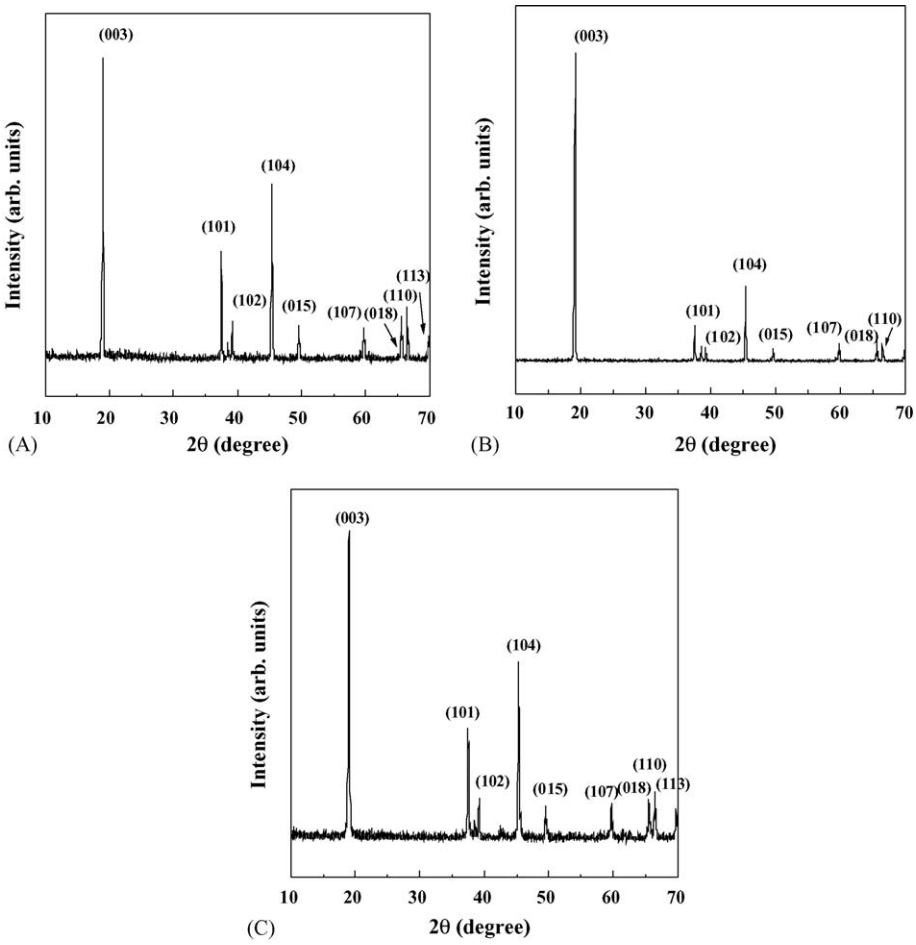

Fig. 2. X-ray diffraction patterns of $LiCoO_2$: (A) commercial powder; (B) manufactured coarse-grained powder; (C) encapsulated with K_2SO_4.

secondary phases or any significant displacement of the main peak positions by the formation of solid solutions. The XRD patterns in Fig. 2 show sharp and well-resolved reflections with perfect crystallographic ordering in all cases.

The charge and discharge curves for Li/$LiCoO_2$ cells at a current rate of *C*/5 over a low operating temperature range (−15 to 0 °C) are given in Fig. 3. The cells fabricated with each type of powder, i.e., commercial micron-sized, synthesized micron-sized and synthesized nanocrystalline powders, are denoted as Cell A, Cell B and Cell C, respectively. For Cell A, the data obtained at 25 °C are displayed together to show the increased discharge capacity at this temperature by the existence of a SEI layer. This will be explained in more detail later. The discharge voltage plateaux of the curves measured in all three cells are almost the same viz., 3.9 V, and the discharge capacities of the cells at 0 °C are of a similar value. Nevertheless closer inspection of the performance at temperatures below 0 °C reveals several differences. For Cell A (Fig. 3A), the discharge capacity at −5 °C is almost the same as the discharge capacity at zero temperature, while the discharge capacity at −10 °C is 91% of that obtained at zero temperature. At −15 °C, the discharge capacity decreases much further. On the other hand, for Cell B (Fig. 3B), the discharge capacity at −10 °C is 98% of that at zero temperature. Also, the reduction of the discharge capacity at −15 °C is less significant than that in the cell fabricated with commercial powder.

It is considered that the difference in discharge capacity in the low-temperature regime may originate from the particle size and specific surface-area. The particle size of the commercial powder ranges from 3 to 6 μm, whereas that of powder obtained without K_2SO_4 encapsulation ranges from 1 to 3 μm. The specific surface-areas are 0.25 and 0.45 $m^{-2}\,g^{-1}$, respectively. This reduced particle size can contribute to the enhanced discharge capacity because it can reduce the mean Li diffusion pathways and increase the contact surface-area between the cathode and the electrolyte. These effects can promote faster ionic transport and contribute to faster charge–discharge processes in secondary lithium batteries [11]. For Cell C, however, the discharge capacity at −10 °C is limited to 93.2% of that at zero temperature. The fact that Cell C has a smaller discharge capacity than that of Cell A or B is possibly due to the existence of the partial cubic spinel phase in the nanocrystalline powder [12] or the lack of the SEI layer which will be explained in more detail later. Nevertheless, the reduction of the discharge capacity at −15 °C is much less than in other cases shown in Fig. 3A and B.

The cycle performance of the Li/$LiCoO_2$ cells at a current rate of *C*/5 and at various low temperatures is given in Fig. 4. As shown in Fig. 4B, the cycle performance of Cell B at −10 °C

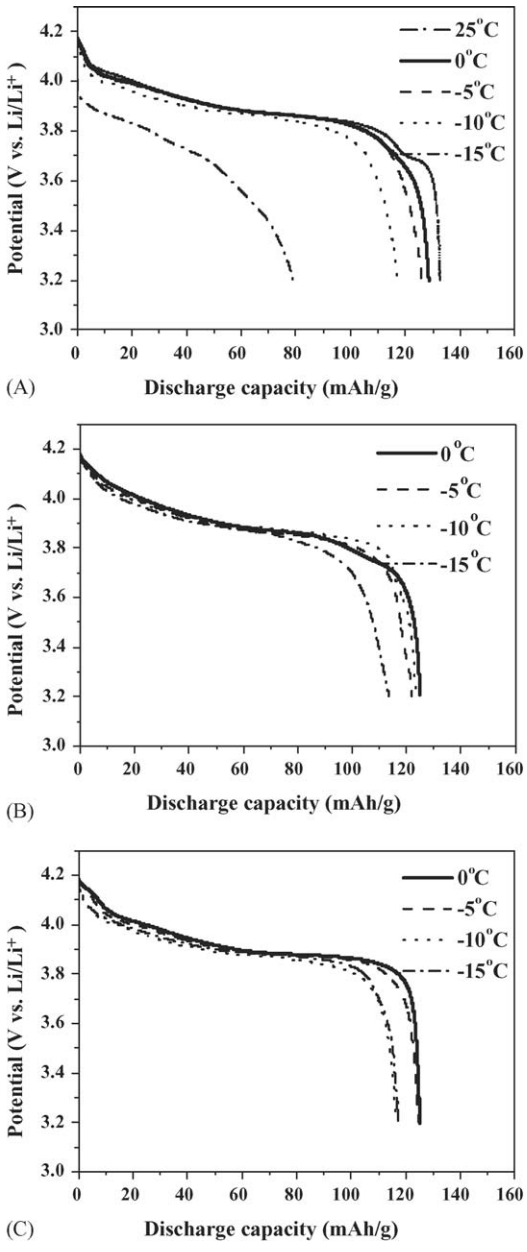

Fig. 3. Low-temperature discharge capacity of Li/$LiCoO_2$ cells made with: (A) commercial powder (Cell A); (B) manufactured coarse-grained powder (Cell B); (C) nanocrystalline powder (Cell C).

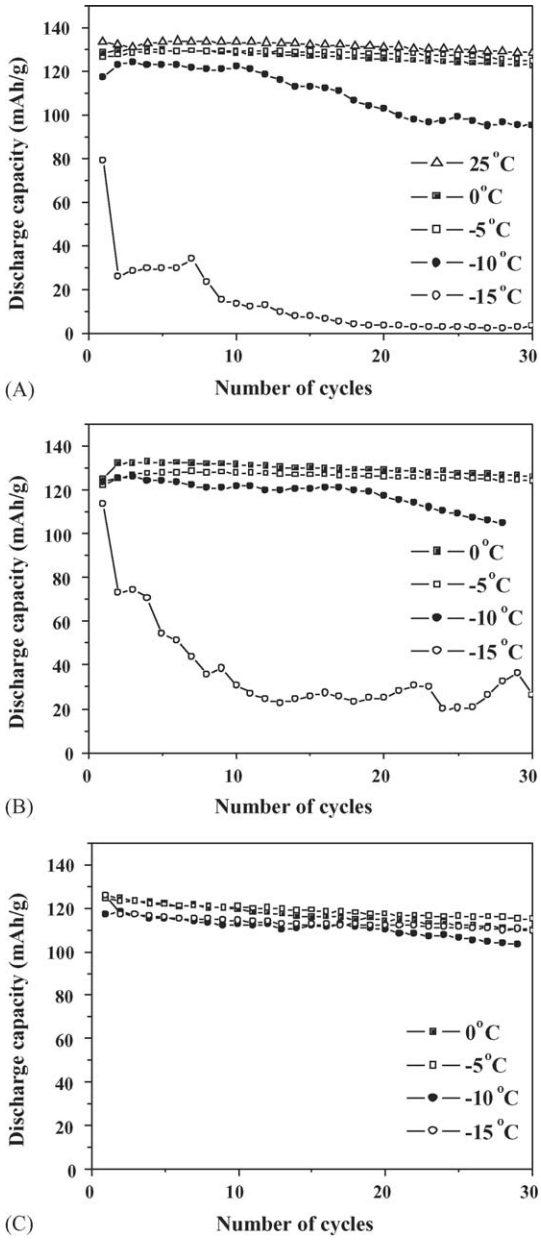

Fig. 4. Low-temperature cycle performance of Li/$LiCoO_2$ cells made with: (A) commercial powder (Cell A); (B) manufactured coarse-grained powder (Cell B); (C) nanocrystalline powder (Cell C).

is improved compared with that of Cell A. It is thought that the smaller particle size and larger specific surface-area contribute also to this enhancement. Moreover, as shown in Fig. 4C, the cycle performance of Cell C is considerably consistent over the low-temperature range. It is thought that the results are due to the further reduction in size of the nanocrystalline powder. In summary, the cell made with nanocrystalline powder exhibits a reliable and consistent performance at low temperature even though the discharge capacity is slightly lower than that of other cells at a given temperature.

To determine the underlying physical reason for the above findings, impedance spectra were measured at room temperature and at −15 °C. The impedance spectrum is generally composed of a straight sloping line in low-frequency region and three partially overlapping semicircles in high-, medium- and low-frequency region. From high to low frequency, the three semicircles can be assigned to the spectra of the cell bulk impedance, the SEI film impedance and the charge-transfer process, respectively [13,14]. Each spectrum can be fitted by an equivalent electric circuit that consists of a resistor and a parallel capacitor. Each component of the resistors is indicated on the impedance spectrum of Cell A shown in Fig. 5A where R_1 and R_2 represent the resistance of the electrolyte and porous electrodes, and R_f is the resistance of the SEI film.

The impedance spectra of the cells in their fully charged states are presented in Fig. 5. When the cells are charged at ambient temperature (Fig. 5A), the electronic resistance of the electrode (R_2) of Cell C is slightly larger than that of Cell A or B.

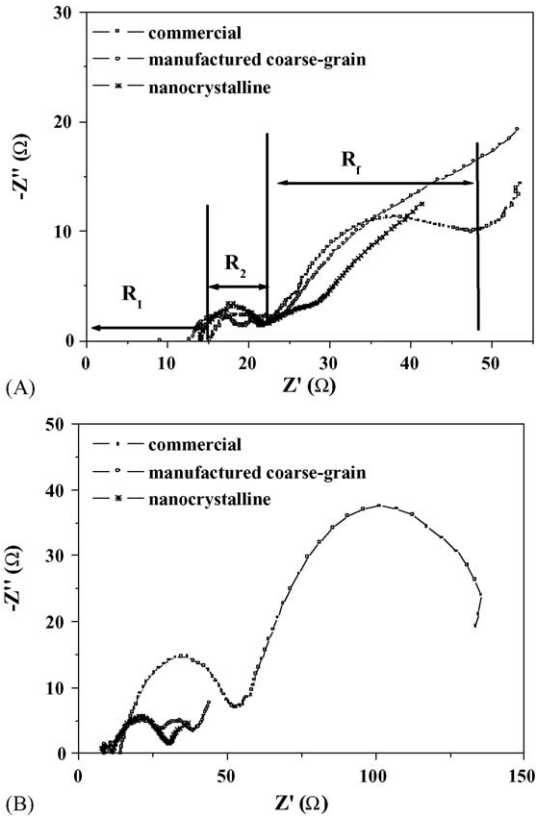

Fig. 5. Impedance curves of Li/$LiCoO_2$ cells at a fully charged state at: (A) room temperature; (B) −15 °C.

This may indicate that the electrical contact between particles is deteriorated due to the small particle size (<100 nm). Also, two semicircles are found in the high- and medium-frequency regions in Cell A, but there is only one semicircle in the high-frequency region in Cell C. This indicates that Cell A has a SEI film layer with a resistance of ∼26 Ω, but Cell C does not have such a layer.

The role of the SEI layer on the cathode has been studied [15–17]. On the basis of XAS results, the presence of LiF compounds in the cathode was inferred when using $LiPF_6$-based electrolytes [17]. The most probable source of the LiF is the decomposition of $LiPF_6$ according to the following reaction [15]:

$$LiPF_6 \rightarrow PF_5 + LiF. \quad (1)$$

The precipitated LiF is most likely the major contributor to the formation of an insulating layer [18]. The precipitation of LiF can affect ionic motion by pore plugging, or it can contribute to the resistive electrical paths in some portions of the cathode structure. Cathodes are generally unstable during organic decomposition of the electrolyte, especially when charged. This instability permits the formation of a dense coating of LiF [17].

A well-defined SEI layer can suppress the decomposition of electrolyte solvents with the help of various additives. The SEI layer can prohibit the leakage of electrolyte solution into the cathode, and thus, improve the cycling performance of lithium-ion batteries [19,20]. Therefore, in the case of the commercial powder, the well-defined SEI layer could be responsible for the higher discharge capacity and the better cycle performance of up to 100 cycles at room temperature, as shown in Figs. 3A and 4A, respectively.

The impedance spectra of cells at −15 °C in their fully charged states are given in Fig. 5B. There are two semicircles at the high- and medium-frequency regions in Cell A but only one semicircle at the high frequency region in Cell C. In the case of Cell B, an additional semicircle appears at the medium-frequency region due to the SEI layer although the SEI film resistance of Cell B has a much smaller value than that of Cell A. In Cell A, the resistance of the SEI film increases from 26 to 81 Ω. If a SEI layer is solely responsible for the discharge

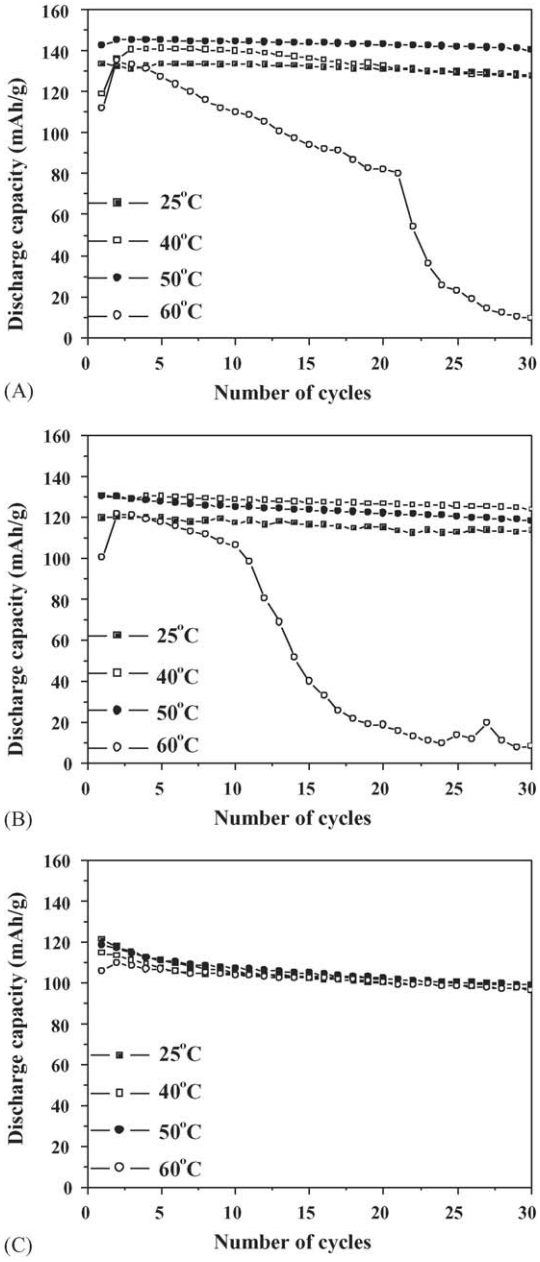

Fig. 6. High-temperature cycle performance of Li/$LiCoO_2$ cells made with: (A) commercial powder (Cell A); (B) manufactured coarse-grained powder (Cell B); (C) nanocrystalline powder (Cell C).

capacity, Cell A should have exhibited a higher discharge capacity at low temperature. In fact, the electronic resistance of the electrode (R_2) increases from 6 to 39 Ω in Cell A so that the discharge capacity of commercial powder is decreased significantly at low temperature. On the other hand, the electrode resistance is remarkably lower in Cell C. This indicates that the increase in electrode resistance is not as significant as in Cell A and thus the low temperature performance is more reliable in Cell C.

The high-temperature cycle performance of the cells at a current rate of *C*/5 is shown in Fig. 6. All cells show the discharge capacity increase up to 50 °C and fairly reliable cycle performances. Except for Cell C, however, the cycle performance deteriorates significantly at 60 °C. During cycling, fatigue of the crystal structure of the active material and decomposition of the electrolyte are accelerated at higher temperatures. The capacity of $LiCoO_2$ might be diminished at an elevated temperature due to microcracks in the $LiCoO_2$ particles induced by phase transformation between the hexagonal and the monoclinic phases. It is considered that the phenomena can be more serious in micron-sized particles. The good cycle performance of Cell C at 60 °C is likely to be due to the small particle size that can be more resistant to mechanical failure.

4. Conclusions

A study has been made of the effect of $LiCoO_2$ particle size on the temperature-dependent performance of Li/$LiCoO_2$ cells. The particle size of the $LiCoO_2$ has been controlled by modifying the powder processing. The discharge capacity of a cell made with nanocrystalline powder is slightly lower than that of cells fabricated with micron-sized powders. This may be due to the lack of a well-formed SEI layer in the cell, which is different behaviour from that of a cell made with commercial micron-sized particles. The cycle performance of a cell made with nanocrystalline $LiCoO_2$ powders is consistent at all operating temperatures and does not deteriorate at the extreme temperature conditions (−15 and 60 °C). It is concluded that the smaller particle size contributes to the enhancement of reliability by increasing the specific surface-area for interclation sites, and by enhancing the resistance to mechanical failure especially at high temperatures.

Acknowledgement

The authors are grateful for R&D support from the National Research Laboratory Program (Development of monolithic high performance battery) of the Korean Government.

References

[1] W.D. Johnston, R.R. Heikes, D. Sestrich, J. Phys. Chem. Solids 7 (1958) 1.
[2] K. Mizushima, P.C. Jones, P.J. Wiseman, J.B. Goodenough, Mater. Res. Bull. 15 (1980) 783.
[3] H.J. Orman, P.J. Wiseman, Acta Crystallogr. C40 (1984) 12.
[4] T.A. Hewston, B.L. Chamberland, J. Phys. Chem. Solids 48 (1987) 97.
[5] C.K. Huang, J.S. Sakamoto, J. Wolfenstine, S. Surampudi, J. Electrochem. Soc. 147 (2000) 2893.
[6] J.P. Feller, G.J. Loeber, S.S. Sandhu, J. Power Sources 81–82 (1999) 867.
[7] J. Shim, R. Kostecki, T. Richardson, X. Song, K.A. Striebel, J. Power Sources 112 (2002) 222.
[8] V.V. Ischenko, O.A. Shlyakhtin, N.N. Oleinikov, et al., Phys. C 282–287 (1997) 855.
[9] Yu.D. Tretyakov, N.N. Oleinikov, O.A. Shlyakhtin, Cryochemical Technology of Advanced Materials, Chapman & Hall, London, 1997, p.195.
[10] O.A. Shlyakhtin, Y.S. Yoon, Y.-J. Oh, J. Eur. Ceram. Soc. 23 (2003) 1893.
[11] J.M. Tarascon, M. Armand, Nature 414 (2001) 359.
[12] S.H. Choi, J.S. Kim, Y.S. Yoon, J. Power Sources 135 (2004) 286.
[13] S.S. Zhang, M.S. Ding, K. Xu, J.L. Allen, T.R. Jow, Electrochem. Solid State Lett. 4 (2001) A206.
[14] S.S. Zhang, K. Xu, T.R. Jow, Electrochem. Solid State Lett. 5 (2002) A92.
[15] Y. Wang, X. Guo, S. Greenbaum, J. Liu, K. Amine, Electrochem. Solid State Lett. 4 (2001) A68.
[16] D. Ostrovskii, F. Ronci, B. Scrosati, P. Jacobsson, J. Power Sources 94 (2001) 183.
[17] M. Balasubramanian, H.S. Lee, X. Sun, X.Q. Yang, A.R. Moodenbaugh, J. McBreen, D.A. Fischer, Z. Fu, Electrochem. Solid State Lett. 5 (2002) A22.
[18] R. Kostecki, X. Zhang, P.N. Ross Jr., F. Kong, S. Sloop, J.B. Kerr, K. Striebel, E. Cairns, F.R. McLarnon, Abstract 190, in: The Electrochemical Society Meeting Abstracts, Vols. 2000-2, Phoenix, AZ, Oct 22–27, 2000.
[19] C. Wang, H. Nakamura, H. Komatsu, M. Yoshio, H. Yoshitake, J. Power Sources 74 (1998) 142.
[20] G.H. Wrodnigg, C. Reisinger, J.O. Besenhard, M. Winter, ITE Battery Lett. 1 (1999) 110.